Inverse Problems in Engineering: Theory and Practice
3rd Int. Conference on Inverse Problems in Engineering
June 13-18, 1999, Port Ludlow, WA, USA

HT07

MONITORING THE WEAR-LINE OF A MELTING FURNACE

Karstein Sørli
SINTEF Applied Mathematics
N-7465 Trondheim NORWAY
Karstein.Sorli@math.sintef.no

Inge M. Skaar
NTNU Mathematical Sciences
N-7491 Trondheim NORWAY
skaar@math.ntnu.no

ABSTRACT

The paper includes a description of different strategies for monitoring the wearline of a melting furnace. This type of industrial monitoring is important for both economic and safety reasons.

Temperature sensors at different locations in the lining of the furnace combined with an inverse heat conduction model are utilized for monitoring the state of the lining. The wearline boundary is represented by a critical isotherm, and the estimation of this isotherm is the crucial part of the inverse solution. Two numerical algorithms for the inverse problem are described.

The algorithms are tested on model data as well as on measurement data acquired at an industrial furnace. One algorithm is based on utilizing a fixed boundary with controlling nodes, on the wearline side, to approximate the measurements. The other algorithmic approach is to approximate the wearline as close as possible with as few curve representing parameters as possible. Both algorithms utilize the common approach of minimizing the sum of the squared residual at the sensor locations.

We also report on some limited numerical sensitivity studies for the algorithms. The numerical experiments confirm the utility of the algorithms as the results are in good agreement with test model data as well as industrial data.

NOMENCLATURE

a_i	parameters of the wearline definition
Δa_i	edge lengths of *hyper-tetrahedrons*
c_i	partial derivatives of u_n w.r.t. a_i
h_a	heat transfer coefficient between steel jacket and air $[W/m^2K]$
h_w	heat transfer coefficient between steel jacket and water $[W/m^2K]$
H	Hessian
J	regulizer
k	thermal conductivity $[W/mK]$
M	$M+1$ is number of wearline definition parameters
N	number of measurement locations
r	spatial coordinate in radial direction $[m]$
u	temperature $[^0C]$
u_a	ambient temperature of air $[^0C]$
u_w	ambient temperature of water $[^0C]$
u_n	computed temperature in location n $[^0C]$
U_n	measured temperature in location n $[^0C]$
v_i	nodal values of temperature along control curve $[^0C]$
x	radial component of approximating cubic
y	axial component of approximating cubic
z	spatial coordinate in vertical direction $[m]$

Greek symbols

α	weighting factor of wearline curvature regularization
α_0	coefficient in regulizer for zero order term
α_1	coefficient in regulizer for first order term
α_2	coefficient in regulizer for second order term
κ	curvature of wearline
Γ	boundary of Ω
Γ_i	boundary segment i of Ω
Ω	region of computed heat conduction
Φ	sum of the squared residual

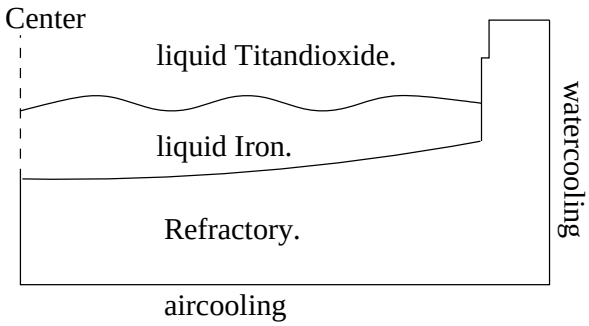

Figure 1. VERTICAL SECTION OF THE MELTER.

INTRODUCTION

The problem origins from an ilmenite melting furnace at Tinfos Titan & Iron KS in Tyssedal, Norway. The products from the melter are iron and titan-dioxide. Because the density of liquid iron is higher than that of liquid titan-dioxide, the slag (titan-dioxide) tap-holes are located above the iron tap-holes. The sidewall of the furnace is water-cooled and the bottom is air-cooled (see Figure 1). In time, the lining of the melter gets worn. This is due to chemical reactions and thermo-mechanical stress. It is crucial that one is able to monitor the wearing to avoid hot metal from breaking through the lining and cause damage to the melter and nearby equipment. Here we consider a rotational symmetric vertical section of the melter as illustrated in Figure 1. In one section there are 24 thermocouples installed to monitor the temperature development. The measurements are also used in a simple model to calculate the position of points on a specific isotherm. The purpose of this paper is to suggest methods to monitor the wearing of the ilmenite melter, i.e. to monitor the position of the wearline. Since we do not know exactly what defines the wearline, we instead try to locate a representative isotherm. Because the melting temperature of the iron is about 1450^oC and that of the titan-dioxide is about 1600^oC, it is certain that the lining is not worn beyond the 1450^oC isotherm. Here we only consider stationary heat conduction. The transients are negligible in our monitoring timeframes. A system is built based on solving inverse steady heat conduction problems repeatedly for several sections of the furnace lining, with a frequency of 1 hour.

MATHEMATICAL MODEL OF HEAT CONDUCTION

The direct problem is to solve a well defined stationary heat conduction problem on a given domain Ω with boundary conditions, see Figure 2. In this specific case one can assume rotational symmetry, i.e.:

$$\frac{1}{r}\frac{\partial}{\partial r}\left(rk(u)\frac{\partial u}{\partial r}\right)+\frac{\partial}{\partial z}\left(k(u)\frac{\partial u}{\partial z}\right)=0 \quad in \quad \Omega \tag{1}$$

where u is the temperature at a point $(r,z)\in\Omega$, r and z being the radial and axial coordinates, respectively. The thermal conductivity, $k(u)$, is generally depending on the temperature. Equation (1) describes heat conduction in cylindrical coordinates when the angular direction component of the conduction is negligible. Even though the furnace lining heat conduction do not satisfy the assumption of axisymmetry in general, this assumption is locally valid and applicable along separate vertical sections of the lining, where a number of thermocouples are located. The boundary Γ of Ω is split in 5 segments, as shown in Figure 2,

$$\Gamma_1\cup\Gamma_2\cup\Gamma_3\cup\Gamma_4\cup\Gamma_5=\Gamma \tag{2}$$

The boundary values for the problem are as follows. On Γ_1 the heat flux is zero, since the model is rotational symmetric,

$$\frac{\partial u}{\partial r}=0 \quad on \quad \Gamma_1 \tag{3}$$

The bottom segment (Γ_2) is air-cooled so we have a mixed condition. The furnace is supplied with fans, blowing air underneath to increase the cooling of the bottom. h_a is the heat transfer coefficient between the bottom and air, and u_a is the ambient air temperature,

$$-k(u)\frac{\partial u}{\partial z}=h_a(u-u_a) \quad on \quad \Gamma_2 \tag{4}$$

The sidewall (Γ_3) is water-cooled so we have a mixed condition here as well. h_w is the heat transfer coefficient between the sidewall and water, and u_w is the ambient water temperature,

$$-k(u)\frac{\partial u}{\partial r}=h_w(u-u_w) \quad on \quad \Gamma_3 \tag{5}$$

At the upper end of the domain, the assumption of insulation is reasonable,

$$\frac{\partial u}{\partial z}=0 \quad on \quad \Gamma_4 \tag{6}$$

At the inside boundary (Γ_5) we have a Dirichlet condition. Because we are trying to monitor the wearline, we choose the function $f(r,z)$ in (7) so as to describe the wearline. For instance, if the melting temperature of the metal inside the furnace is 1450^oC we choose the function to be equal to this melting temperature. In (Radmoser, 1998) a similar approach is used.

$$u=f(r,z) \quad on \quad \Gamma_5 \tag{7}$$

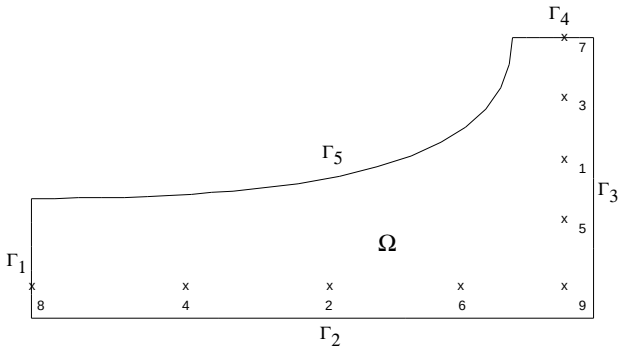

Figure 2. THE HEAT CONDUCTING REGION WITH CURVED WEARLINE. MEASUREMENT LOCATIONS ARE SHOWN.

Another possible modeling approach is to consider the problem as an inverse multi-dimensional free boundary problem. This is quite natural for phase change problems. In (Katz & Rubinsky, 1984) and (Zabaras et al., 1988) such approaches are considered for the one-dimensional case.

ALGORITHMS FOR INVERSE HEAT CONDUCTION

The unknown wearline denoted by Γ_5, will be estimated utilizing a finite number of measurements

$$U_n, \qquad n = 1, \ldots, N \tag{8}$$

at given locations in Ω, in combination with solving the mathematical model of heat conduction governed by Equations (1)-(7). The locations used in our studies are shown in Figure 2, i.e. a maximum of 9 sensor locations. The actual number of sensors in vertical sections of the industrial furnace is larger.

Many authors, e.g. (Beck et al.,1985), (Hensel, 1991), have analyzed inverse heat conduction problems, both analytically and numerically. In (Sorli & Olden, 1998) a method for finding heat transfer coefficients, based on a bisection type algorithm for nonlinear and implicit equations, is presented. In (Radmoser, 1998) a similar problem to the present one is formulated and solved by a special type of angle constraint to regularize the problem.

In this section we present two different numerical algorithms for solving the given inverse problem. Both methods are based on the common approach of minimizing the sum of the squared residual at the measurement points,

$$\min \sum_{n=1}^{N} (u_n - U_n)^2 \tag{9}$$

This function is refined by regularization term(s) that are described in the following subsections.

Method of control boundary

The idea is that since we do not know exactly what the domain for the boundary-value problem looks like we just assume some fixed shape for the unknown boundary (Γ_5). We define this boundary as the *control boundary*. A rule is that the control boundary should be chosen such that it is as close to the desired isotherm as possible. This can be achieved by some a priori calculations or by starting with a very simple control boundary, e.g. a straight line and improve the guess from the results in an iterative manner. The inverse problem then reads: Find a temperature distribution along the control boundary which reconstructs the measured temperatures at the sensor positions. That is, given measurements U_n, $n = 1, \ldots, N$, where N is the number of thermocouples, find a Dirichlet condition on Γ_5 which minimizes the sum of squares as given in (9). The values u_n, $n = 1, \ldots, N$, are the calculated temperatures at the thermocouple locations for a given temperature distribution along Γ_5. Since inverse problems tend to be *ill-posed* it is not very likely that we will succeed in minimizing the square sum and get a reasonable solution to our problem. It is easily seen that the problem has similarities to the sideways heat equation which is ill-posed, that is, the solution does not depend continuously on the data, see (Beck et al.,1985) and (Hensel, 1991). To limit the behavior of the temperature distribution along Γ_5 we introduce a regulizer in addition to the square sum, see (Radmoser, 1998) and (Hensel, 1991). Therefore, instead of minimizing the pure square sum we minimize

$$\Phi(v_1, v_2, .., v_m) = \sum_{n=1}^{N} (u_n - U_n)^2 + J \tag{10}$$

with respect to the unknown boundary values v_i, $i = 1, \ldots, m$. The term J is a *regulizer* and m is the number of nodes along the fixed control boundary. In calculations presented here J is a finite difference approximation to

$$\alpha_0 \int_{\Gamma_5} (u)^2 d\gamma + \alpha_1 \int_{\Gamma_5} \left(\frac{\partial u}{\partial \Gamma} \right)^2 d\gamma + \alpha_2 \int_{\Gamma_5} \left(\frac{\partial^2 u}{\partial \Gamma^2} \right)^2 d\gamma \tag{11}$$

where α_0, α_1 and α_2 are constants. This type of regularization is referred to as Tikhonov regularization in literature, see (Beck et al.,1985) and (Engl, Hanke & Neubauer, 1996). The constants are chosen large enough to stabilize the problem so iterations will converge. There exist a theory on how to determine optimal values for the constants, see (Engl, Hanke & Neubauer, 1996). If it should happen that our guess for the control line is nearly on the wanted isotherm, the extra term J becomes small. This fact encourages us to make a good guess for the control line. To solve the modified minimization problem we use the method of Newton-Raphson. See (Dennis & Schnabel, 1983) for details on this method and optimization methods in general.

Using Newton-Raphson we have to solve

$$F(v_1, v_2, .., v_m) = \begin{bmatrix} \frac{\partial \Phi(v_1, v_2, .., v_m)}{\partial v_1} \\ \frac{\partial \Phi(v_1, v_2, .., v_m)}{\partial v_2} \\ \vdots \\ \frac{\partial \Phi(v_1, v_2, .., v_m)}{\partial v_m} \end{bmatrix} = 0 \qquad (12)$$

Using Newton-Raphson we have to calculate the Jacobian of F which is given by

$$H = \begin{bmatrix} \frac{\partial^2 \Phi(v_1, v_2, .., v_m)}{\partial v_1^2} & \frac{\partial^2 \Phi(v_1, v_2, .., v_m)}{\partial v_1 \partial v_2} & \dots & \frac{\partial^2 \Phi(v_1, v_2, .., v_m)}{\partial v_1 \partial v_m} \\ \frac{\partial^2 \Phi(v_1, v_2, .., v_m)}{\partial v_2 \partial v_1} & \frac{\partial^2 \Phi(v_1, v_2, .., v_m)}{\partial v_2^2} & \dots & \frac{\partial^2 \Phi(v_1, v_2, .., v_m)}{\partial v_2 \partial v_m} \\ \vdots & \vdots & \ddots & \vdots \\ \frac{\partial^2 \Phi(v_1, v_2, .., v_m)}{\partial v_m \partial v_1} & \frac{\partial^2 \Phi(v_1, v_2, .., v_m)}{\partial v_m \partial v_2} & \dots & \frac{\partial^2 \Phi(v_1, v_2, .., v_m)}{\partial v_m^2} \end{bmatrix} \qquad (13)$$

and is symmetric. One advantage of the control boundary method is that the Jacobian becomes independent of the boundary values along Γ_5 when the thermal heat conductivity is independent of temperature. That is, we do only need to calculate the Jacobian once. This will of course result in very fast convergence for the Newton-Raphson iterations, because we in fact are trying to solve a linear problem. The method of solving for unknown boundary values for linear systems are presented in (Hensel, 1991). The Newton-Raphson updates becomes

$$\mathbf{v}_{i+1} = \mathbf{v}_i - H^{-1}(\mathbf{v}_i) F(\mathbf{v}_i) \qquad (14)$$

where $\mathbf{v}_i = [v_1, v_2, .., v_m]_i^T$.

Test cases Two test cases, one with a “minor wearline” and one with a “severe wearline”, were created to test the algorithm. Table 1 shows the computed temperatures at the probe locations for both cases. Remember that wearline in this case is represented by the 1450^oC isotherm.

The upper plot of Figure 3 shows the calculated wearline, the actual wearline and the control line. In this case we tried to reconstruct a minor wearline using a linear control line rather far from the actual wearline, both in location and shape. The lower plot of Figure 3 shows the relative error at the locations of the thermocouples. The numbering of the thermocouples in Table 1 are as in Figure 2. The constants in the regulizer term were chosen to be $\alpha_0 = 0.0$, $\alpha_1 = 0.0005$ and $\alpha_2 = 0.0003$.

In Figure 4 the same wearline as in Figure 3 is reconstructed, but this time using a better fitted curved control line. Comparing the relative errors plotted in the lower plot of Figure 3 and 4

Table 1. SIMULATED TEMPERATURES AT NINE PROPE LOCATIONS FOR TEST CASE 1 (”MINOR” WEAR) AND TEST CASE 2 (”SEVERE” WEAR).

n	r_n	z_n	U_n (1)	U_n (2)
1	6.50	2.00	305.40	404.87
2	3.75	0.50	384.99	506.14
3	6.50	2.75	480.66	672.39
4	2.00	0.50	480.92	646.39
5	6.50	1.25	189.36	242.92
6	5.25	0.50	268.55	347.69
7	6.50	3.50	667.25	872.56
8	0.00	0.50	550.63	804.88
9	6.50	0.50	98.61	125.80

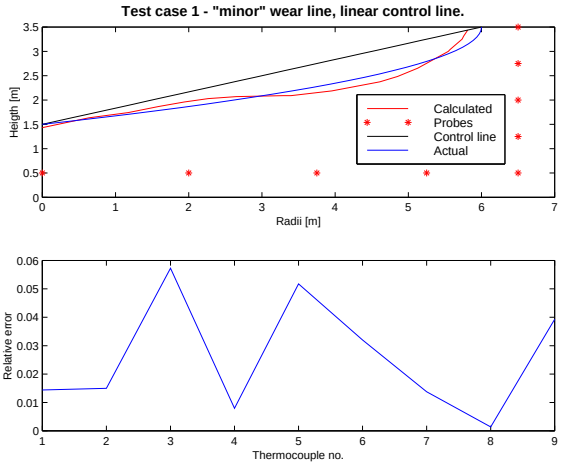

Figure 3. RECONSTRUCTION OF MINOR WEARLINE WITH LINEAR CONTROL LINE.

shows that a control line closer to the wearline, both with respect to shape and location, will contribute to a solution which fits the measured temperatures better. The same values for the regularization parameters as in the linear control curve case have been used to reconstruct the wearline in Figure 4.

For Case 2, i.e. “severe wearline”, the same tests have been performed. In Figure 5 a linear control line has been used in the reconstruction of the temperature distribution giving relative errors as in the lower plot of the Figure 5 . Again, same values as before have been used for the regularization parameters.

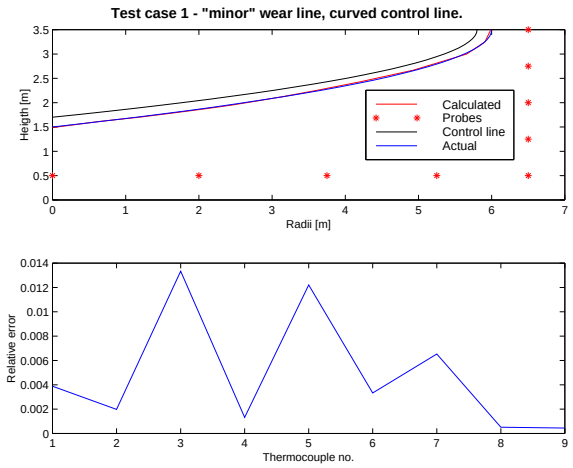

Figure 4. RECONSTRUCTION OF MINOR WEARLINE WITH CURVED CONTROL LINE.

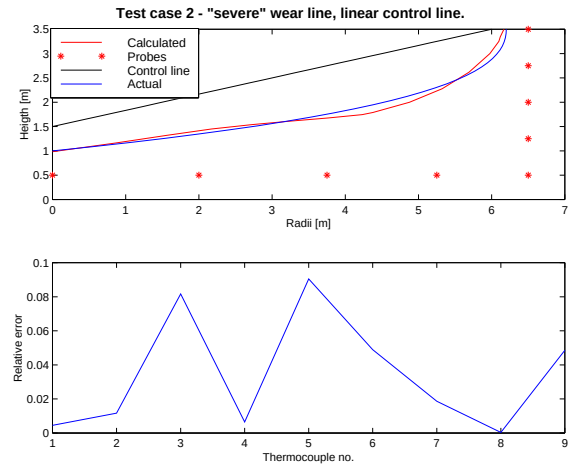

Figure 5. RECONSTRUCTION OF SEVERE WEARLINE WITH LINEAR CONTROL LINE.

We have also in the case of "severe wearline" tried to reconstruct the temperature distribution using a curved control line which is closer in location and shape to the critical isotherm. As was the case for the "minor wearline" this results in a better fit to measured temperatures, which is shown in the lower plot of Figure 6.

A brief response analysis To analyze the response of temperature at measurement locations we introduced perturbations of the location of the boundary Γ_5. In this case the boundary

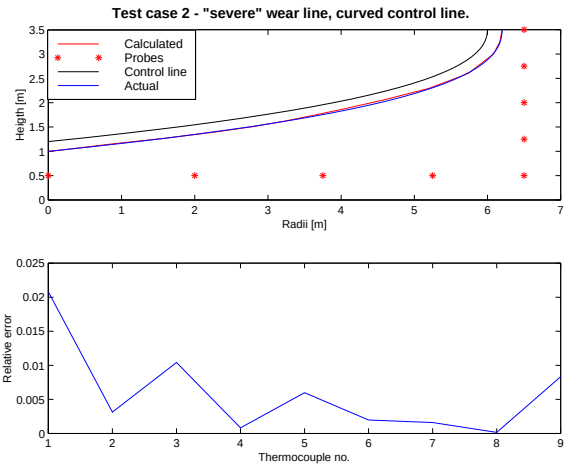

Figure 6. RECONSTRUCTION OF SEVERE WEARLINE WITH CURVED CONTROL LINE.

condition for the inner boundary is $u = 1450^oC$. The conditions for the other boundaries are the same as for the test cases. The inner boundary is described by quadratic polynomial

$$z(r) = c_0 + c_1 r + c_2 r^2 \tag{15}$$

The constants c_i, $i = 0,1,2$, are determined from the equations

$$\frac{dz}{dr}(r_2) = 0, \quad z(r_1) = z_1 \quad \text{and} \quad z(r_2) = z_2 \tag{16}$$

Then the temperatures at probe locations, $n = 1,\ldots,9$, were simulated with $(r_1,z_1) = (0.0,1.5)$ and $(r_2,z_2) = (6.0,3.5)$. Now, to test how perturbations of the location of the isotherm (inner boundary) would effect the measured temperatures at probe locations, we simulated two cases. Case 1 with $(r_1,z_1) = (0.0,1.5+0.025)$ and $(r_2,z_2) = (6.0-0.0025,3.5)$, which is a curve just above the original. Case 2 with $(r_1,z_1) = (0.0,1.5-0.025)$ and $(r_2,z_2) = (6.0+0.0025,3.5)$, which is a curve just under the original curve.

In Figure 7 the two curves above and under the middle curve are given in the upper plot and corresponding relative errors (response) at probe locations in the lower plot. This shows that the relative errors in the test cases, at least for the curved control lines, are acceptable. That is, if one can tolerate deviations as in Figure 7.

Isotherm Cubic Curve Approximation

In this case the unknown location of an isotherm representing or approximating the wearline, is estimated in an iterative

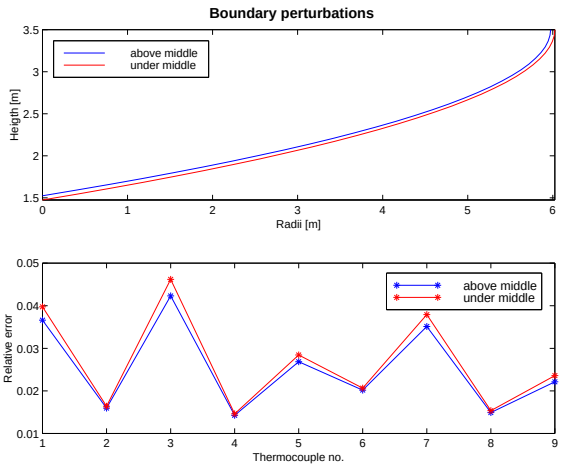

Figure 7. RELATIVE ERROR FOR SMALL PERTURBATIONS OF ISOTHERM POSITION.

manner. First we formulate the algorithm with no other regularization than a parametric representation of this critical isotherm. This wearline parameterization is a special kind of regularization of the problem since we limit the number of parameters for describing the curve. Later we extend the regularization by including a curvature term to the minimization problem.

Smooth wearlines As suggested we apply the well-known concept of minimizing the sum of the squared residuals (9) at the N measurement points. One approach of solving this problem could be to use the *multidimensional downhill simplex method* (Nelder & Mead, 1965). This method only requires function evaluations, not derivatives. However, it is not very efficient in terms of the number of function evaluations it requires. Therefore, we have formulated another method based on the assumption of *local* linear dependence

$$u_n(a_1,\ldots,a_M) = c_0^n + c_1^n a_1 + \cdots + c_M^n a_M \tag{17}$$

between the computed values u_n and M curve parameters $a_1,\ldots,a_M$ defining the critical and unknown isothermal curve. In this work we have limited our study to *cubic curves* and present results for this case. However, extensions to *cubic splines* are proposed for problems with wearlines that are changing quite rapidly on some parts.

In (17), for $n = 1,\ldots,N$ the coefficients c_m^n, $m = 0,\ldots,M$, are determined by multidimensional interpolation. $M+1$ different sets of parameter values $\{a_1^j,\ldots,a_M^j\}$, $j = 0,\ldots,M$, give the following linear system of algebraic equations

$$\begin{bmatrix} 1 & a_1^0 & \cdots & a_M^0 \\ 1 & a_1^1 & \cdots & a_M^1 \\ \vdots & \vdots & \ddots & \vdots \\ 1 & a_1^M & \cdots & a_M^M \end{bmatrix} \begin{bmatrix} c_0^n \\ c_1^n \\ \vdots \\ c_M^n \end{bmatrix} = \begin{bmatrix} u_n^0 \\ u_n^1 \\ \vdots \\ u_n^M \end{bmatrix} \tag{18}$$

which may be solved by Gaussian elimination with backsubstitution or any triangular decomposition scheme. Observe that (18) must be solved for N different right-hand side vectors $\left[u_n^0,\ldots,u_n^M\right]^T$, $n = 1,\ldots,N$. However, the coefficient matrix is the same in each case. Therefore, the elimination only needs to be done once, while the backsubstitution is required for each of the different right-hand side vectors.

In the present study the parameter values $\{a_1^j,\ldots,a_M^j\}$, $j = 0,\ldots,M$, are given by

$$\mathbf{a}^0 = \left[a_1^0,\ldots,a_M^0\right]^T \tag{19}$$

$$\mathbf{a}^j = \mathbf{a}^0 + \Delta a_j \mathbf{e}_j^T, \qquad j = 1,\ldots,M \tag{20}$$

forming right-angled *hyper-tetrahedrons* with $M+1$ vertices in the M-dimensional Euclidean space. In the last equation (20) Δa_j is the edge length of the tetrahedron in the direction of $\mathbf{e}_j = [0,\ldots,0,1,0,\ldots,0]$ where 1 is in the j^{th} position of the vector.

Let $\mathbf{a}^0$ be our latest estimate of the curve parameters. We use an iterative formula to compute a new and improved estimate from the previous one. To solve the minimization problem of (9), the approach of computing the partial derivatives of this expression, with respect to $\{a_j\}$, $j = 1,\ldots,M$ in this case, and setting the results equal to zero, is a common approach of finding the values minimizing a given function. In doing so we get

$$f_m(a_1,\ldots,a_M) \equiv \sum_{n=1}^{N} (u_n - U_n)\, c_m^n = 0, \qquad m = 1,\ldots,M \tag{21}$$

where $c_m^n = \frac{\partial u_n}{\partial a_m}$, $m = 1,\ldots,M$, $n = 1,\ldots,N$, are given by (18). We solve this system iteratively by the well-known Newton-Raphson formula

$$\begin{bmatrix} \frac{\partial f_1}{\partial a_1} & \frac{\partial f_1}{\partial a_2} & \cdots & \frac{\partial f_1}{\partial a_M} \\ \frac{\partial f_2}{\partial a_1} & \frac{\partial f_2}{\partial a_2} & \cdots & \frac{\partial f_2}{\partial a_M} \\ \vdots & \vdots & \ddots & \vdots \\ \frac{\partial f_M}{\partial a_1} & \frac{\partial f_M}{\partial a_2} & \cdots & \frac{\partial f_M}{\partial a_M} \end{bmatrix} \begin{bmatrix} \Delta a_1^0 \\ \Delta a_2^0 \\ \vdots \\ \Delta a_M^0 \end{bmatrix} = - \begin{bmatrix} f_1 \\ f_2 \\ \vdots \\ f_M \end{bmatrix} \tag{22}$$

where both the right-hand side vector and the coefficient matrix are computed for $\mathbf{a} = \mathbf{a}^0$. The new iterate for the curve parameters is

$$\mathbf{a}^0 = \mathbf{a}^0 + \Delta\mathbf{a}^0$$

where $\Delta\mathbf{a}^0 = \left[a_1^0, \ldots, a_M^0\right]^T$.

In order to reduce computing time we have split the iteration in two different cycles; one inner iteration cycle and one outer. During an inner iteration cycle we do not relocate $\mathbf{a}^j$, $j = 1, \ldots, M$, but iterates only on $\mathbf{a}^0$. In the outer iteration, however, we do relocate the other parameter sets. The strategy we have chosen for ending an inner iteration cycle and doing an outer iteration step, is based on computing the distance from $\mathbf{a}^0$ to the *hyperplane* spanned by $\mathbf{a}^j$, $j = 1, \ldots, M$. If this distance is larger than some prescribed limit, and the number of inner iterations of the present cycle is below some limit, the inner iteration continues. When one of the limits is reached, the present inner iteration cycle stops, and an outer iteration is executed. The new $\mathbf{a}^j$, $j = 1, \ldots, M$, parameter sets are still determined by (20), but now the Δa_j hyper-tetrahedron edge lengths are set to half the lengths of the previous ones. The latter choice may seem arbitrary, but it has proved to be quite efficient in the numerical tests we have done so far. However, it may prove more efficient to relate the reduction rate of the edge lengths of the hyper-tetrahedrons to the function values evaluated.

Any finite element or finite volume solver for direct heat conduction problems can be utilized for computing the u_n, $n = 1, \ldots, N$, for given parameter sets $\{a_1, \ldots, a_M\}$, i.e. for fixed Γ_5 (see Figure 2). In our validation tests a finite element solver and a triangular mesh generator were used. The main requirement of the solver is that it should handle curved boundaries sufficiently well. The mesh generator should create a quality mesh relatively fast since the mesh has to be regenerated several times for different regions. A typical mesh is shown in Figure 8. The mesh is refined towards Γ_5 due to the large temperature gradients close to this curve. The meshing is based on the Delaunay-Voronoi triangulation algorithm (see e.g. (Carey, 1997)).

Test cases - knowing the shape of the wearlines Here we present results of using the algorithm presented above. The test regions are shown in Figure 9.

The cases (a) and (b) of Figure 9 are chosen so as to represent two extreme wear scenarios. They do not reflect real wear in existing industrial furnaces. Both these artificial wearlines are created by a cubic curve of the form

$$\mathbf{x}(s) = \mathbf{b}_0 + \mathbf{b}_1 s + \mathbf{b}_2 s^2 + \mathbf{b}_3 s^3, \qquad 0 \le s \le 1 \qquad (23)$$

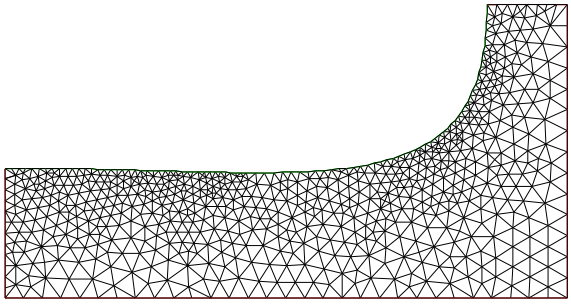

Figure 8. TRIANGULAR MESH FOR A GIVEN WEARLINE.

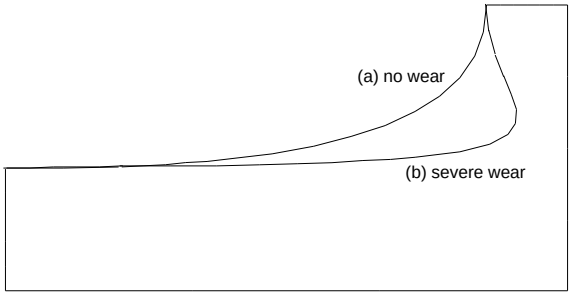

Figure 9. TEST REGIONS WITH SMOOTH WEARLINES.

where

$$\mathbf{b}_0 = \mathbf{x}(0) \qquad (24)$$
$$\mathbf{b}_1 = \mathbf{x}'(0) \qquad (25)$$
$$\mathbf{b}_2 = -3\left[\mathbf{x}(0) - \mathbf{x}(1)\right] - 2\mathbf{x}'(0) - \mathbf{x}'(1) \qquad (26)$$
$$\mathbf{b}_3 = 2\left[\mathbf{x}(0) - \mathbf{x}(1)\right] + \mathbf{x}'(0) + \mathbf{x}'(1) \qquad (27)$$

This type of curve is often called *Ferguson* cubic curves (see e.g. (Davies & Samuels, 1996)). In the tests the following assumptions are made

$$\mathbf{x}'(0) = (a_1, 0) \qquad (28)$$
$$\mathbf{x}'(1) = (0, a_2) \qquad (29)$$
$$\mathbf{x}(0) = (0, a_3) \qquad (30)$$
$$\mathbf{x}(1) = (a_4, H) \qquad (31)$$

i.e., the slope of the wearline is horizontal at the left side and vertical at the right side of it. These are reasonable assumptions in real wear scenarios. In (31) H is the height of the furnace wall. It is set equal to 3.5 in both tests. Also, in both cases $a_2 = 5, a_3 = 1.5$ and $a_4 = 6$. In case (a) $a_1 = 10$, while $a_1 = 26$ in the severe wear case (b).

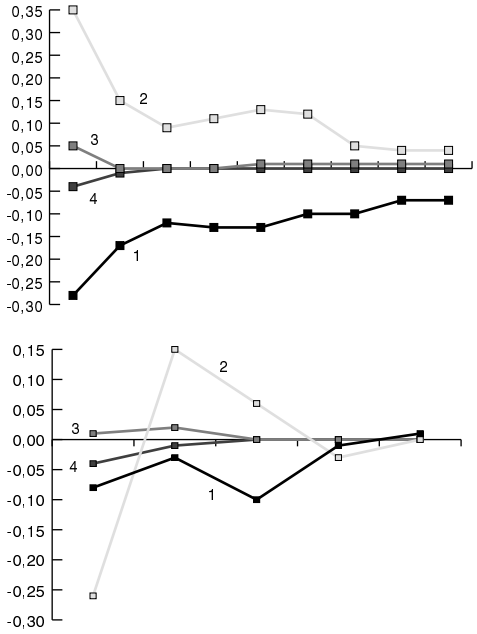

Figure 10. $a_i^c - a_i^e$, $i = 1, \ldots, 4$, AS FUNCTIONS OF NUMBER OF OUTER ITERATIONS. NO WEAR CASE IN UPPER AND WEAR CASE IN LOWER FIGURE (c=COMPUTED, e=EXACT).

The direct problem of (1) was solved for these two cases by a finite element solver. Numerical results were stored in positions 1 to 9 as depicted in Figure 2. These numbers were subsequently treated as measurements. This completes the preparation of the model tests.

The test of the given solution algorithm for the inverse problem is now concerned with estimating the wearlines of Figures 9a and 9b, using the same type of curve for estimating the wearline. However, now the parameters a_1 to a_4 are not known and will be estimated by the inverse algorithm. Hopefully, we are able to create the same parameter sets. Of course, this task is much easier than the real problem when the shape of the wearline is not known a priori. However, the test is still valuable, since it must succeed on this type of problem in order to handle arbitrary wearlines. The results of the tests are presented in Figure 10. Observe that the algorithm needs more iterations to converge for the no wear case than for the wear case. The reason is mainly that the cubic curve in the study is not very well suited for approximation of the wearline in this case. It is slightly better for the severe wear case. However, for heavy wear it would probably be better to use cubic splines instead of a single cubic. This will be investigated in future.

The maximum relative error of the computed values at the measurement points is in this case less than 1% after only a couple of outer iterations (see description above). The initial estimates were chosen to enclose the exact parameter set with an initial *hyper-tetrahedron* having edge lengths of 10% of the absolute value of the exact parameters.

Modification for nonsmooth wearlines We modify the algorithm with extra regularization as claimed at the beginning of this subsection. The reason for the modification is the need for handling real furnace wearlines which in general are not smoothly shaped. For such cases the previous algorithm will easily fail to converge, due to sensitivity of the algorithm to *disturbances on the wearline*. This argument could also be turned around by saying that the algorithm is sensitive to disturbances in the measurements. The latter is obviously the case in real life, since every thermocouplebased measuring system produce data with some degree of noise. A rigorous analysis of this matter is not done, but is planned in future work.

We have tested a modification of the algorithm based on the following minimization problem

$$\min \left(\sum_{n=1}^{N} (u_n - U_n)^2 + \alpha \int_0^1 \kappa(s) ds \right) \tag{32}$$

Here κ is the *curvature* of the wearline

$$\kappa(s) = (\mathbf{x}_{ss} \cdot \mathbf{x}_{ss})^{1/2}$$

and α is some weighting factor. Assuming a cubic wearline as in (23), its curvature is given by

$$\kappa^2(s) = 2\mathbf{b}_2 \cdot \mathbf{b}_2 + 6\mathbf{b}_2 \cdot \mathbf{b}_3 s + 9\mathbf{b}_3 \cdot \mathbf{b}_3 s^2$$

For the case of the 4-parametric problem formulated above the system of algebraic equations given in (21) is modified as

$$\widehat{f}_1 \equiv \sum_{n=1}^{N} (u_n - U_n)\, c_1^n + \alpha(4a_1 - 6a_4) = 0 \tag{33}$$

$$\widehat{f}_2 \equiv \sum_{n=1}^{N} (u_n - U_n)\, c_2^n + \alpha(4a_2 + 6a_3 - 21) = 0 \tag{34}$$

$$\widehat{f}_3 \equiv \sum_{n=1}^{N} (u_n - U_n)\, c_3^n + \alpha(6a_2 + 12a_3 - 42) = 0 \tag{35}$$

$$\widehat{f}_4 \equiv \sum_{n=1}^{N} (u_n - U_n)\, c_4^n + \alpha(12a_4 - 6a_1) = 0 \tag{36}$$

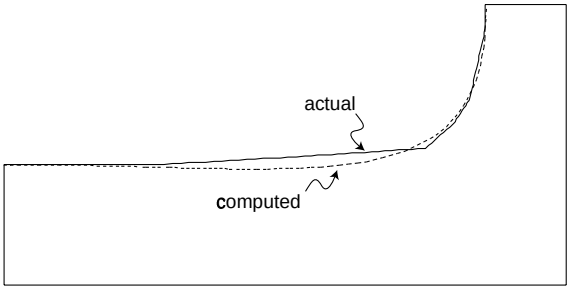

Figure 11. COMPUTED AND ACTUAL WEARLINES.

For the 4-parametric case the Newton iteration matrix of (22) is modified as

$$\begin{bmatrix} \frac{\partial f_1}{\partial a_1}+4\alpha & \frac{\partial f_1}{\partial a_2} & \frac{\partial f_1}{\partial a_3} & \frac{\partial f_1}{\partial a_4}-6\alpha \\ \frac{\partial f_2}{\partial a_1} & \frac{\partial f_2}{\partial a_2}+4\alpha & \frac{\partial f_2}{\partial a_3}+6\alpha & \frac{\partial f_2}{\partial a_4} \\ \frac{\partial f_3}{\partial a_1} & \frac{\partial f_3}{\partial a_2}+6\alpha & \frac{\partial f_3}{\partial a_3}+12\alpha & \frac{\partial f_3}{\partial a_4} \\ \frac{\partial f_4}{\partial a_1}-6\alpha & \frac{\partial f_4}{\partial a_2} & \frac{\partial f_4}{\partial a_3} & \frac{\partial f_4}{\partial a_4}+12\alpha \end{bmatrix} \tag{37}$$

Test cases - not knowing the shape of the wearlines In the following tests we are not assuming any knowledge of the shape of the wearlines except for the following assumptions

$$y'(0) = x'(1) = 0 \tag{38}$$

i.e., the wearline is horizontal at the left side and vertical at the right hand side, as in the previous case. The computed wearline is compared to the actual wearline in Figure 11.

Different values of α were chosen and the respective history of iterations is shown in Figure 12. Numerical experiments indicate that α should be larger than 0.5 in this case in order to get convergent results. For other wearlines and regions this value may change.

The maximum relative error of the computed values at the measurement points is in this case about 3%. The initial estimates were chosen to enclose the exact parameter set with an initial *hyper-tetrahedron* having edge lengths of 10% the absolute value of the exact parameters.

RESULTS ON FURNACE DATA

In this section we present simulations of the wearline using actual temperature measurements from an ilmenite melting furnace. This is done with the method of control boundary. The method is tested on two different sets of measurements at different acquisition dates. There are some effects which can cause

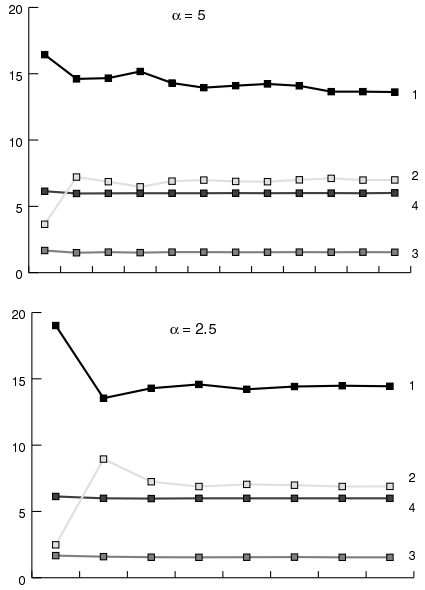

Figure 12. $a_i^c, i = 1, \ldots 4,$ AS FUNCTIONS OF NUMBER OF OUTER ITERATIONS.

differences in comparison to measured temperatures other than the method itself. One effect is that the heat transfer coefficients are assumed to be $h_a = 30$ and $h_w = 150$ which is close to their actual values but not quite correct. Other contributions to error may be inaccuracy in location of thermocouples and air gaps in the brick-work. In Figure 13 the wearline is calculated using a linear control boundary. As expected the relative errors at the probe locations are rather large. But this calculation gives guidelines to how the position and shape of the control line should be. If the control line is placed closer to the actual wearline as in Figure 14 for the same set of measurements, we can observe some reduction in the relative errors. To get a better idea of how the actual wearline looks like, more effort should be made to get the control line closer to the wearline. This should be done because the relative errors are still too large. We can observe a special effect in the upper part of the lining in Figure 14. This is caused by frozen titan-dioxide at the inside of the lining. This is a wanted effect because it protects the refractory against chemical attacks. Iron is not that easily frozen along the lining. One would have to increase the cooling of the sidewall significantly to get this effect. One gets in a position where one would have to consider lining wear against heat loss. In Figure 15 the method of control line has been tested on another set of measured temperatures.

In the two cases presented in this section there is no reason to believe that any of the original refractory materials have been worn. The cases have been picked relatively early in the lifetime of the furnace lining. This lining has been operative for only a short period of time. The lifetime of such a lining should be

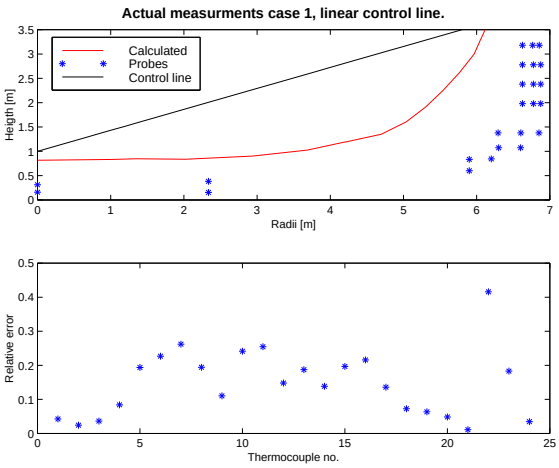

Figure 13. CALCULATED WEARLINE USING LINEAR CONTROL LINE FOR CASE 1.

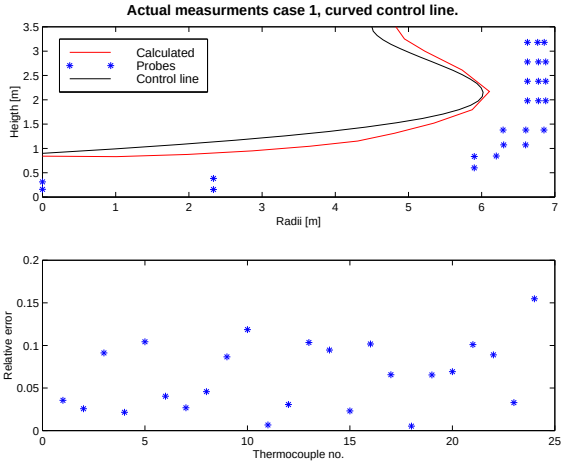

Figure 14. CALCULATED WEARLINE USING CURVED CONTROL LINE FOR CASE 1.

somewhere between 15 and 20 years. At this stage there is no reason to believe that the lining should not reach its expected lifetime.

CONCLUSION

Numerical models for monitoring the wearline of the lining of a melting furnace have been developed. Two algorithms for solving the resulting inverse heat conduction problem are presented and tested, both on test problem data and on real measurement data sampled in an industrial furnace. Numerical experiments confirm the utility of both *the control boundary algorithm* and *the algorithm of isotherm curve approximation*. The reliability of the former one depends on the average distance between the curve and the actual wearline.

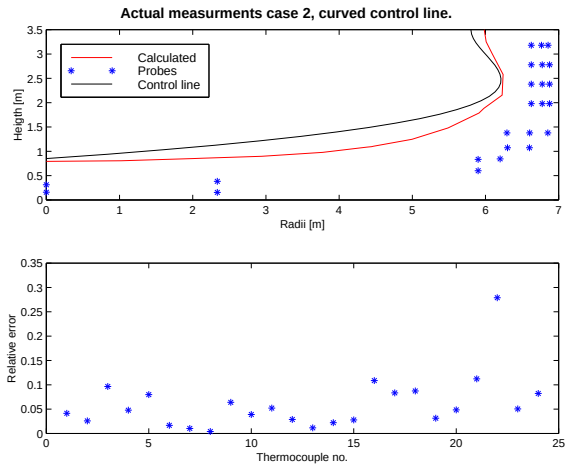

Figure 15. CALCULATED WEARLINE USING CURVED CONTROL LINE FOR CASE 2.

The tests of the control boundary method on minor and severe wearlines, show that if the control curve corresponds reasonably well to the actual wearline in location and shape, the relative errors become less than 2.5% in both cases. This is well within the acceptable bounds found in the response analysis. Since the control line can be relocated in an iterative manner to improve location and shape, this can be achieved in most cases.

The isotherm cubic curve approximation produces results comparable to results of the ”close version” of the control boundary algorithm. The method requires limited knowledge of the actual wearline shape. Therefore, it is better suited to handle inverse problems with a complex behavior like rapidly changing wearlines. The algorithm probably needs a modification for the most severe cases, and the utilization of splines are suggested. This will be investigated in future work.

Both algorithms need extra regularization terms when applied to real wearline problems. The control boundary algorithm adds regularization using common constraints on the temperature along the control boundary, i.e. Tikhonov regularization. The modified algorithm of isotherm cubic curve approximation includes a constraint on the curvature of the isotherm approximation, i.e. another type of Tikhonov regularization . These modifications are shown to be both necessary and successful in numerical experiments.

The regularization term and the improving effects of locating the control line closer to the isotherm imply that the method

of control boundary should be implemented as an iterative search for the isotherm. If that can be achieved, the regularization term vanish if the control line is exactly at the isotherm and we would only be minimizing the squared sum involving calculated and measured temperatures at probe locations.

Both methods as presented in this paper, are stand-alone methods for solving inverse heat conduction with an unknown boundary like the wearline in the present problem. However, an interesting possibility is to use the method of fixed control boundary as a refinement method after using the method of isotherm approximation by cubics or splines. The potential of these ideas will be investigated in future work.

ACKNOWLEDGMENT

This work was supported by Tinfos Titan and Iron KS (TTI), Ferrolegeringsindustriens Forskningsforening (FFF), Holta's Legat, and SINTEF. Special thanks to G. Folmo at TTI for supplying valuable information and guidance concerning this work. Also we would like to thank H. E. Krogstad and S. P. Nørsett for valuable discussions.

REFERENCES

Beck, J.V., Blackwell, B.F., and St. Clair, C.R., *Inverse Heat Conduction - Ill-Posed Problems*, John Wiley and Sons, New York, 1985.

Carey, G.F., *Computational Grids - Generation, Adaptation and Solution Strategies*, Taylor & Francis, 1997.

Davies, A. and Samuels, P., *An Introduction to Computational Geometry for Curves and Surfaces*, Clarendon Press, Oxford, 1996.

Dennis, Jr., J. E. and Schnabel, R. B., *Numerical Methods for Unconstrained Optimization and Nonlinear Equations*, Prentice Hall, New Jersey, 1983.

Engl, H. W., Hanke, M. and Neubauer, A., *Regularization of Inverse Problems* Kluwer Academic Publishers, 1996.

Hensel, E., *Inverse Theory and Applications for Engineers*, Prentice Hall, New Jersey, 1991.

Katz, M. A. and Rubinsky, B., *An Inverse Finite-Element Technique to Determine the Change of Phase Interface Location in One-Dimensional Melting Problems*, Numer. Heat Transfer, Vol. 7, pp. 269-283, 1984.

Nelder, J. A. and Mead, R., *A Simplex Method for Function Minimization*, Computer Journal, Vol. 7, pp. 308-313.

Radmoser, E., *Security-Related Parts of a Blast Furnace Model*, ECMI Newsletter, No 23, March 1998.

Sørli, K. and Olden, V., *Numerical Estimation of Heat Transfer and Thermal Stresses in Water Cooling of Shipbuilding Profiles*, Proceedings of ASME IMECE'98, Symposium on Numerical and Experimental Methods in Heat Transfer, Vol. 5, pp. 183-190, Anaheim, CA, November 1998.

Zabaras, N., Mukherjee, S. and Richmond, O., *An Analysis of Inverse Heat Transfer Problems With Phase Changes Using an Integral Method*, ASME J. Heat Transfer 110, pp. 554-561, 1988.